Generation of novel oncolytic vaccinia virus with improved intravenous efficacy through protection against complement-mediated lysis and evasion of neutralization by vaccinia virus-specific antibodies

Namhee Lee,[1] Yun-Hui Jeon,[2,3] Jiyoon Yoo,[2,3] Suk-kyung Shin,[2,3] Songyi Lee,[1] Mi-Ju Park,[1] Byung-Jin Jung,[1] Yun-Kyoung Hong,[1] Dong-Sup Lee [ID] ,[2,3] Keunhee Oh[1]

For numbered affiliations see end of article.

Correspondence to
Professor Dong-Sup Lee;
dlee5522@snu.ac.kr

Dr Keunhee Oh;
khoh@kr.sillajen.com

ABSTRACT

Background Oncolytic virus immunotherapy has revolutionized cancer immunotherapy by efficiently inducing both oncolysis and systemic immune activation. Locoregional administration has been used for oncolytic virus therapy, but its applications to deep-seated cancers have been limited. Although systemic delivery of the oncolytic virus would maximize viral immunotherapy's potential, this remains a hurdle due to the rapid removal of the administered virus by the complement and innate immune system. Infected cells produce some vaccinia viruses as extracellular enveloped virions, which evade complement attack and achieve longer survival by expressing host complement regulatory proteins (CRPs) on the host-derived envelope. Here, we generated SJ-600 series oncolytic vaccinia viruses that can mimic complement-resistant extracellular enveloped virions by incorporating human CRP CD55 on the intracellular mature virion (IMV) membrane.

Methods The N-terminus of the human CD55 protein was fused to the transmembrane domains of the six type I membrane proteins of the IMV; the resulting recombinant viruses were named SJ-600 series viruses. The SJ-600 series viruses also expressed human granulocyte-macrophage colony-stimulating factor (GM-CSF) to activate dendritic cells. The viral thymidine kinase (*J2R*) gene was replaced by genes encoding the CD55 fusion proteins and GM-CSF.

Results SJ-600 series viruses expressing human CD55 on the IMV membrane showed resistance to serum virus neutralization. SJ-607 virus, which showed the highest CD55 expression and the highest resistance to serum complement-mediated lysis, exhibited superior anticancer activity in three human cancer xenograft models, compared with the control Pexa-Vec (JX-594) virus, after single-dose intravenous administration. The SJ-607 virus administration elicited neutralizing antibody formation in two immunocompetent mouse strains like the control JX-594 virus. Remarkably, we found that the SJ-607 virus evades neutralization by vaccinia virus-specific antibodies.

WHAT IS ALREADY KNOWN ON THIS TOPIC

⇒ Systemic administration of oncolytic vaccinia virus has been limited due to the rapid clearance of injected virus by the complement and innate immune systems.

WHAT THIS STUDY ADDS

⇒ Our new oncolytic vaccinia virus platform expressing human CD55 protein on its membrane, prolonged viral survival by protecting against complement-mediated lysis and by evading neutralization by vaccinia virus-specific antibodies.

HOW THIS STUDY MIGHT AFFECT RESEARCH, PRACTICE OR POLICY

⇒ Our novel oncolytic vaccinia virus platform can be treated systemically and repeatedly and thus may expand the target cancer profile to include deep-seated cancers and widespread metastatic cancers.

Conclusion Our new oncolytic vaccinia virus platform, which expresses human CD55 protein on its membrane, prolonged viral survival by protecting against complement-mediated lysis and by evading neutralization by vaccinia virus-specific antibodies; this may provide a continuous antitumor efficacy until a complete remission has been achieved. Such a platform may expand the target cancer profile to include deep-seated cancers and widespread metastatic cancers.

INTRODUCTION

Oncolytic virus (OV) immunotherapy has revolutionized cancer immunotherapy. Through selective infection and replication in cancer cells, as well as the induction of immunogenic cancer cell death, OVs efficiently induce both oncolysis and systemic

immune activation.[1] OVs can convert immunologically cold tumors into hot tumors, and they do not require baseline intratumoral T-cell infiltration before treatment[2–4]; thus, they can be applied in combination with anti-programmed cell death protein-1/programmed death ligand-1 therapies.[2–7]

OVs have primarily been applied through locoregional administration.[2 8–10] Local immunotherapy constitutes a rational approach to minimize systemic toxicity, as well as an in situ vaccination platform that may facilitate homing of activated cancer-specific T cells into tumor tissue.[11–14] However, intralesional injections are applied to superficially located cancers; although image-guided injection into deep-seated cancers is possible, the injection of an adequate dose is dependent on the technical ability of the physician.[8 15 16] The heterogeneous nature of cancer also requires simultaneous targeting of individual cancer cell variants.[17–19] Therefore, systemic delivery is an important goal in the field of OVs, which would allow access to disseminated and heterogeneous tumor deposits.[7 15 16 20] However, systemically administered viruses are rapidly removed from circulation by the complement and innate immune systems.[21 22]

Infected cells produce some vaccinia viruses (VACVs; 5%–20%) as extracellular enveloped virions, which evade complement attack and achieve longer survival by expressing host complement regulatory proteins (CRPs) on the host-derived envelope.[23–26] Notably, most VACVs (80%–95%) are produced as intracellular mature virions (IMVs), which lack surface CRPs and are therefore susceptible to complement-mediated lysis that reduces bioactivity.[24–26]

Here, we generated SJ-600 series oncolytic VACVs that can mimic complement-resistant extracellular enveloped virions through the incorporation of human CRP CD55 on the IMV membrane; this was achieved by combining human CD55 with the transmembrane domains of VACV membrane proteins.[27 28] SJ-600 series oncolytic VACVs expressing human CD55 on the IMV membrane showed resistance to serum virus neutralization. SJ-607 virus, which showed the highest level of CD55 expression and the greatest resistance to serum complement-mediated lysis, demonstrated good anticancer efficacy after single-dose intravenous treatment. SJ-607 virus showed increased anticancer activity in cell-derived xenograft models, compared with the control Pexa-Vec (JX-594) virus,[29 30] after single-dose intravenous administration. Additionally, SJ-607 virus showed better therapeutic efficacy after intravenous administration than intratumoral administration. The administration of the SJ-607 virus elicited neutralizing antibody (NAb) formation in two immunocompetent mouse strains like the control JX-594 virus. Remarkably, we found that the SJ-607 virus evades neutralization by VACV-specific antibodies. These observations indicated that our novel virus expressing human CRP CD55 on the IMV membrane can act as a novel OV platform to enable systemic and repeated treatment by providing resistance to serum complement attack and

evading neutralization by VACV-specific antibodies; thus, it will expand the target cancer profile to include deep-seated cancers and widespread metastatic cancers.

MATERIALS AND METHODS
Cell culture
MDA-MB-231, HCT-116, AGS, SK-MEL-2, SNU-1214, SNU-333, SNU-475, SW620, and HeLa cells were obtained from Korean Cell Line Bank (Seoul, Korea). U-2-OS, A549, and H1975 cells were obtained from the American Type Culture Collection (Manassas, Virginia, USA). HeLa, U-2-OS, A549, and NCI-H1975 cells were grown in Dulbecco's Modified Eagle Medium; all other cell lines were grown in Roswell Park Memorial Institute Medium (RPMI)-1640 supplemented with 10% fetal bovine serum.

SJ-600 series virus construction
The flanking sequences of thymidine kinase (*J2R*) and the genes encoding human granulocyte-macrophage colony-stimulating factor (GM-CSF) and VACV outer membrane proteins were amplified by PCR, using JX-594 as the template. The human CD55 sequence was amplified from a commercial plasmid (Sino Biological, Beijing, China). Recombinant virus was constructed using a standard homologous recombination protocol.[31] The *GM-CSF* and *CD55* genes were placed under the control of the VACV synthetic early/late promoter and synthetic late promoter, respectively.[32] All viruses were amplified in HeLa cells and purified by 36% sucrose cushion centrifugation, in accordance with the standard protocol.[33]

Flow cytometry
U-2-OS cells were infected at a multiplicity of infection (MOI) of 0.5 and harvested 16 hours post-infection. The infected cells were fixed, permeabilized, and stained with anti-CD55 antibody (#67; Invitrogen, Carlsbad, California, USA) (1:250); they were then incubated with Alexa Fluor 594-conjugated secondary antibody (Invitrogen) (1:1000). CD55 expression was detected by LSRFortessa (BD Biosciences, Franklin Lakes, New Jersey, USA) and analyzed with FlowJo software.

Western blotting analysis
Protein from purified virions was separated in pre-casted SDS-PAGE 4–15% gels (Bio-Rad, Hercules, California, USA) by electrophoresis and transferred onto nitrocellulose membranes in Trans-Blot SD Cell (Bio-Rad). The membranes were stained with anti-CD55 (#NaM16-4D3; Santa Cruz Biotechnology, Santa Cruz, California, USA) (1:200), anti-VACV A27 (#NR-627; BEI Resources, Manassas, Virginia, USA) (1:5000), and anti-β-actin (#BA3R; Invitrogen) (1:1000) antibodies, then incubated with appropriate horseradish peroxidase-conjugated secondary antibodies (1:5000). In deglycosylation experiments, lysed virions were treated with Protein Deglycosylation Mix (New England Biolabs, Ipswich, Massachusetts USA) and analyzed with antibodies to CD55, VACV A27,

and β-actin. Blots were imaged using Davinch-Chemi CAS-400 (Davinch-K, Seoul, Korea).

Immunofluorescence imaging

U-2-OS cells were infected at an MOI of 5 for 12 hours; they were then fixed, permeabilized, and incubated with anti-CD55 (#67; Invitrogen) (1:1000) and anti-VACV A27 (#ab35219; Abcam, Cambridge, UK) (1:1000) antibodies. Next, cells were incubated with Alexa Fluor 488-conjugated (Abcam) (1:1000) and Alexa Fluor 594-conjugated (Jackson ImmunoResearch, West Grove, Pennsylvania, USA) (1:1000) secondary antibodies, as well as 4′,6′-diamidino-2-phenylindole (DAPI) (Invitrogen); images were obtained by confocal microscopy (STELLARIS 8; Leica Microsystems, Wetzlar, Germany).

Transmission electron microscopy

Purified virions were incubated with anti-CD55 antibody (#NaM16-4D3; Santa Cruz) (1:50), then with 12 nm colloidal gold-conjugated antibody (Jackson ImmunoResearch) (1:20). Grids were negatively stained with NanoVan (Nanoprobes, Yaphank, New York, USA) and imaged by transmission electron microscopy at 120 kV (JEM-1400; JEOL, Tokyo, Japan).

In vitro viral stability in human serum

SJ-600 series viruses were mixed with commercially available normal human serum (HS) (Sigma-Aldrich, Darmstadt, Germany) to a final serum dilution of 20%. U-2-OS cells were incubated with virus for 3 days (until plaques formed). In subsequent experiments, cells were infected with virus in the presence of 20% or 50% HS. The numbers of plaques were compared with the numbers obtained from control cells.

In vitro cytotoxicity

Ten human cancer cell lines were infected with serially diluted virus for 72 hours. Cell Counting Kit-8 (CCK-8) solution (Dojindo, Kumamoto, Japan) was added, and the absorbance at 450 nm (A_{450}) was measured using a Microplate Absorbance Reader (Tecan, Mannedorf, Switzerland).

Experimental animals

NOD.Cg-Prkdc^{scid} IL2rg^{tm1Wjl}/SzJ (NSG) mice (Jackson Laboratory, Bar Harbor, Maine, USA) and C57BL/6 and BALB/c mice (Koatech, Pyeongtaek, Korea) were maintained under specific pathogen-free conditions at Seoul National University Animal Facility (Seoul, Korea).

In vivo antitumor efficacy studies

HCT-116, A549, or MDA-MB-231 cells were subcutaneously implanted into NSG mice. When tumor volume reached 80–120 mm^3, mice underwent intravenous administration of a single dose of virus at a high dose (HD, 5×10^6 pfu) or low dose (LD, 1×10^6 pfu) via the tail vein. Tumor growth was monitored two times weekly and the volume was calculated as follows: volume=length×width^2×0.5.

In vivo biodistribution and histological analysis

Mice carrying HCT-116 xenografts underwent intravenous administration of 1×10^6 pfu of virus; the presence of virus was monitored using an imaging system (IVIS Lumina X5; PerkinElmer, Waltham, Massachusetts, USA). Mice carrying A549 xenografts underwent intravenous administration via tail vein of 1×10^6 pfu of virus. After 120 hours, tumor tissues were excised, fixed, and cut into 50 μm-thick sections; they were then stained with anti-CD31 antibody (#2H8; Millipore, Billerica, Massachusetts, USA) (1:100), followed by Cy3-conjugated antibody (Jackson ImmunoResearch) (1:400) and DAPI. Samples were imaged by confocal microscopy (Zeiss LSM 980; Carl Zeiss, Oberkochen, Germany); positive areas were analyzed using ZEN Blue software (Carl Zeiss).

VACV-reactive antibody formation and titration of neutralizing activity

BALB/c and C57BL/6 mice were intravenously injected via tail vein with single or multiple doses of virus at 5×10^6 pfu. In the multiple dosing groups, viruses were administered weekly three times. Blood was collected prior to the first dose of virus, then collected once weekly five times.

VACV-reactive antibodies were measured by ELISA method. Briefly, intact virus was coated on the plate and heat-inactivated virus-treated mouse serum was treated as primary antibody. Detection was performed using Horseradish Peroxidase (HRP)-conjugated anti-mouse IgG antibody (Invitrogen) (1:1000) at 450 nm to quantitate the total antibodies reactive to the coated virus. To measure the neutralizing activity by VACV-reactive antibodies, heat-inactivated mouse serum was incubated with virus, transferred onto cultures of U-2-OS cells, and incubated for 3 days. NAb titer$_{50}$ was defined as the reciprocal of the highest dilution of serum that resulted in cell viability ≥50%.

Statistical analysis

Statistical analyses were performed using GraphPad Prism V.8.0 (GraphPad Software, San Diego, California, USA). Comparisons between two groups were performed using two-tailed unpaired Student's t-tests. Group comparisons of tumor growth were performed by two-way analysis of variance, followed by Bonferroni's post hoc test. In all analyses, $p<0.05$ was considered indicative of statistical significance.

RESULTS

Construction of oncolytic VACV incorporating human CD55 on the IMV membrane

SJ-600 series oncolytic VACVs were designed to incorporate human CRP CD55 on the membranes of IMVs,[24] thereby protecting the viruses from complement-mediated attack during circulation after intravenous administration.

To incorporate human CD55 protein on the membranes of IMVs, the N-terminus of the CD55 protein containing

Table 1 List of SJ-600 series viruses used in this study

Virus	Descriptive name	VV gene deactivation (recombination site)	CD55 expression	VV TM used for CD55 expression	VV TM a.a. position	Marker genes
JX-594	VV-GM-CSF	J2R	No	N/A	N/A	LacZ
SJ-610	VV-GM-CSF	J2R	No	N/A	N/A	Luc-GFP
SJ-601	VV-GM-CSF-CD55 D8	J2R	Yes	D8L	276–304	Luc-GFP
SJ-604	VV-GM-CSF-CD55 A16	J2R	Yes	A16L	343–377	Luc-GFP
SJ-605	VV-GM-CSF-CD55 F9	J2R	Yes	F9L	176–212	Luc-GFP
SJ-606	VV-GM-CSF-CD55 G9	J2R	Yes	G9R	320–340	Luc-GFP
SJ-607	VV-GM-CSF-CD55 H3	J2R	Yes	H3L	285–324	Luc-GFP
SJ-608	VV-GM-CSF-CD55 L1	J2R	Yes	L1R	184–250	Luc-GFP

All viruses were derived from the Wyeth strain of vaccinia virus and all expressed GM-CSF. An expression cassette including GM-CSF was inserted into the thymidine kinase (*J2R*) gene of the vaccinia genome to inactivate this gene. The *CD55* gene was fused with the transmembrane domain of one of the vaccinia virus membrane proteins, as indicated.
GFP, green fluorescent protein; GM-CSF, granulocyte-macrophage colony-stimulating factor; LacZ, β-galactosidase; Luc, luciferase; N/A, not applicable; TM, transmembrane domain; VV, vaccinia virus.

the signal peptide and four functional sushi domains without the glycosylphosphatidylinositol (GPI) anchor (a.a. 1–352) was fused to the transmembrane domains of the IMV membrane proteins. More than 20 IMV membrane proteins have been identified; they are involved in viral attachment and entry into target cells.[34] Among them, six type I transmembrane proteins (A16, D8, F9, G9, H3, and L1) were selected as fusion partners for human CD55 (table 1). Recombinant VACVs expressing human CD55 fused with each of the six membrane proteins were designated as SJ-601 and SJ-604 through SJ-608; these viruses were designated SJ-600 series oncolytic VACVs. All SJ-600 series viruses also expressed human GM-CSF to activate dendritic cells.[32] Through homologous recombination, the viral thymidine kinase (*J2R*) gene was replaced by genes encoding the CD55 fusion proteins and GM-CSF (online supplemental figure 1).

Confirmation of the expression of human CD55 on SJ-600 series OVs

The expression of CD55 by SJ-600 series recombinant VACVs was evaluated by flow cytometry analysis of virus-infected U-2-OS cells. Cells infected with the control JX-594 virus, in which only GM-CSF was recombined with the J2R region, were used as negative controls (table 1).[32] Although CD55 was not detected in cells infected with JX-594, all cells infected with SJ-600 series viruses expressed human CD55 protein; the highest level of CD55 expression was detected in cells that had been infected with SJ-607 virus (figure 1A,B). These observations indicated that the N-terminus of CD55 protein fused to the transmembrane domains of IMV membrane proteins was expressed as expected.

To determine whether the virus itself expressed human CD55 protein, total protein was extracted from purified IMVs and CD55 expression was detected by western blotting analysis. The VACV A27 protein and β-actin were used as internal controls for viral and cell-derived proteins, respectively. Two forms of human CD55 proteins were expressed by SJ-600 series viruses, with molecular weights of 50 kDa and 70 kDa

depending on the glycosylation status (figure 1C); this glycosylation effect was confirmed by removing most N-linked and O-linked oligosaccharides from glycoproteins via treatment with Deglycosylation Enzyme Mix (figure 1D). The total expression levels and differential expression patterns of the two forms of CD55 varied among the SJ-600 series viruses; the SJ-605 and SJ-607 viruses showed particularly high expression of the 70 kDa form (figure 1C).

To visualize the expression of CD55 on IMVs, U-2-OS cells infected with SJ-607, which showed the strongest CD55 expression among the SJ-600 series viruses, were evaluated by confocal microscopy. First, U-2-OS cells were infected with SJ-607 or control JX-594 virus for 12 hours. After infected cells had been stained with anti-CD55 antibody, anti-A27 antibody, and DAPI, they were evaluated by confocal microscopy. Cells infected with either JX-594 or SJ-607 exhibited extensive DAPI staining of nucleic acids in the perinuclear cytoplasm, which coincided with the site of expression of A27, the VACV envelope protein (figure 1E). The DAPI/A27-stained region in the cytoplasm adjacent to the nucleus may represent a 'virus factory,' where VACVs are produced and accumulate through intensive viral DNA replication. CD55 protein expression was observed in this virus factory area in cells that had been infected with SJ-607 but not with JX-594 (figure 1E). These findings indicated that CD55 protein was specifically expressed in SJ-607 viral particles.

Surface expression of CD55 protein on the viral membrane is necessary for the virus to avoid damage from the activated complement system during systemic circulation. Immunoelectron microscopic analysis was performed to confirm CD55 incorporation on the viral membrane. Purified SJ-607 and JX-594 viral particles were adsorbed onto carbon-coated grids, sequentially stained with anti-human CD55 antibody and secondary antibody conjugated
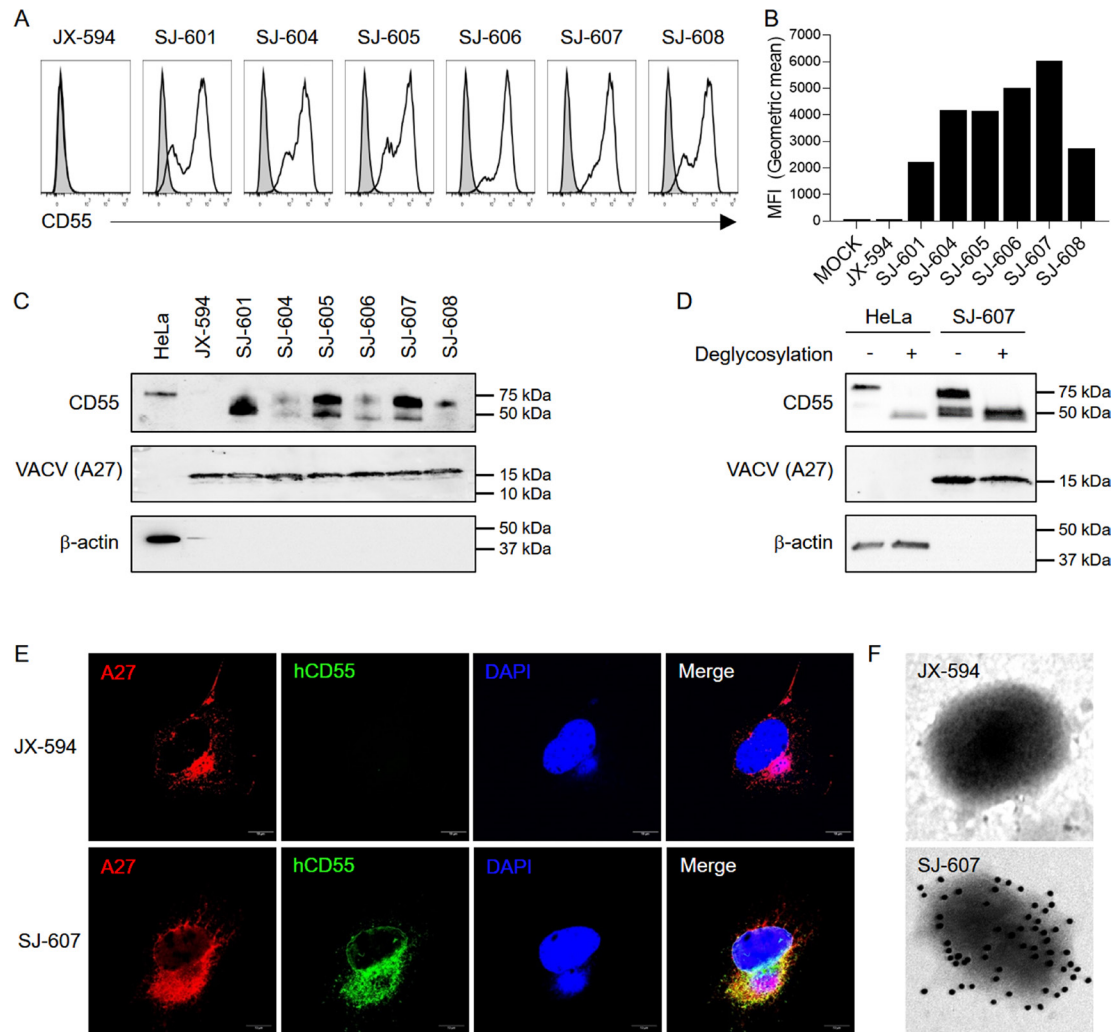
Figure 1 Confirmation of CD55 expression on SJ-600 series viruses. (A, B) Flow cytometry analysis of SJ-600 series virus-infected cells. U-2-OS cells were infected with virus at an MOI of 0.5, and CD55 expression was analyzed by flow cytometry at 16 hours post-infection. Representative (A) histogram and (B) mean fluorescence intensity levels showed CD55 expression on infected cells, compared with negative control cells. (C) CD55 expression on purified virions was confirmed by western blotting. Aliquots of 1 µg of viral protein were loaded and the presence of target protein was determined using antibodies to CD55, VV-A27, and β-actin. Protein bands were 70–75 kDa (CD55), 14 kDa (VV-A27), and ~42 kDa (β-actin). HeLa cell lysate was used as a positive control, and JX-594 was used as a negative control. (D) Deglycosylation of CD55. SJ-607 virion lysates treated with or without deglycosylases were analyzed by western blotting using antibodies to CD55, VV-A27, and β-actin. HeLa cell lysate was used as a control. (E) Immunofluorescence analysis of SJ-607-infected U-2-OS cells. Cells were infected at an MOI of 5 for 12 hours, then labeled with anti-VV-A27 antibody (red), anti-CD55 antibody (green), and DAPI. All images were visualized by confocal fluorescence microscopy. Representative and merged images are shown. Scale bar, 10 µm. (F) Transmission electron microscopy of purified virus. Purified virions were adsorbed onto carbon-supported nickel grids and incubated with mouse antibody against CD55, then incubated with 12 nm gold-conjugated anti-mouse IgG. The figure shows a representative image of CD55 on the surface of the viral membrane. DAPI, 4′,6′-diamidino-2-phenylindole; MFI, mean fluorescence intensity; MOI, multiplicity of infection; VACVs, vaccinia viruses.

with 12 nm gold particles, and evaluated by transmission electron microscopy. Gold particles bound to human CD55 protein were densely localized on the surface of SJ-607 viral particles, whereas no gold particles were observed on the surface of JX-594 viral particles (figure 1F). Taken together, these findings showed that human CD55 protein was selectively incorporated on the IMV membrane of SJ-600 series OVs as designed; among them, SJ-607 virus had the highest level of surface CD55 protein incorporation.

CD55 incorporation on the membrane of SJ-600 series OVs protects against complement attack

To determine whether oncolytic VACVs incorporating CD55 protein on the membrane are resistant to complement-mediated lysis, the SJ-600 series viruses were incubated with HS and functional virus titer was evaluated by plaque assays.[33] Briefly, the numbers of plaques formed in U-2-OS cells were counted after infection with SJ-600 series viruses or control JX-594 virus; all viruses had been preincubated with 20% normal HS. The resultant
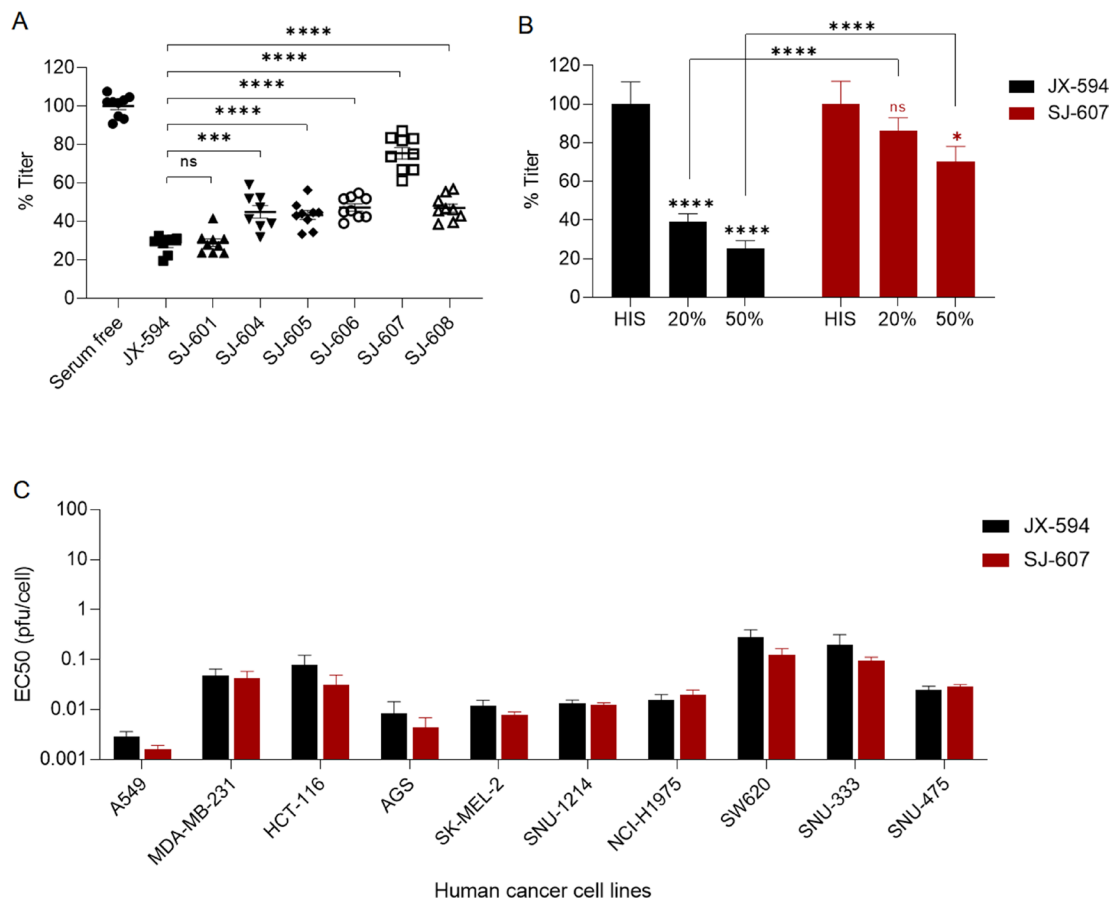
Figure 2 Sensitivities of SJ-600 series viruses to neutralization by complement in human serum. (A) CD55-expressing viruses were incubated with 20% human serum for 2 hours, then used to inoculate U-2-OS cells and incubated for 3 days to allow plaque formation. The numbers of plaques obtained are expressed as percentages of the number of plaques obtained with the serum-free control. (B) JX-594 and SJ-607 were incubated in the presence of 20% and 50% human serum. The numbers of plaques obtained are expressed as percentages of the number of plaques obtained with 50% heat-inactivated human serum. Data represent means±SD of three measurements. Differences between means were analyzed using unpaired Student's t-tests. *P<0.05, **p<0.01, ***p<0.001, ****p < 0.0001, ns=ns, not significant (p>0.05). HIS, heat-inactivated serum. (C) In vitro cytotoxicity of SJ-607. Potency of SJ-607 compared with JX-594 in various human cancer cell lines. EC_{50} was measured by Cell Counting Kit-8 assays at 72 hours post-infection. Values are shown as means±SD of pooled data from four experiments performed in triplicate.

viral titer of JX-594 virus, which did not express human CD55, decreased to approximately 28.1% in the presence of 20% HS, compared with the serum-free control. With the exception of SJ-601, the SJ-600 series viruses showed ≥1.5-fold serum stability, compared with JX-594 virus (figure 2A). In particular, SJ-607 virus exhibited 75.5% survival in the presence of 20% HS; the stability of SJ-607 virus in the presence of HS was 2.7-fold better than the stability of JX-594 virus (figure 2A).

To directly confirm that the maintenance of a higher SJ-600 series virus titer in HS (compared with JX-594 virus) was the result of complement resistance mediated by CD55 incorporation on the viral membrane, heat-inactivated serum was used as a negative control. Additionally, the concentrations of heat-inactivated serum and HS were also increased up to the experimental limit of 50% to better approximate physiological conditions. The titers of JX-594 virus decreased to 39.0% and 25.1% in the presence of 20% and 50% HS, respectively,

compared with titers in the presence of heat-inactivated serum (figure 2B, left panel). In contrast, the titer of SJ-607 virus decreased to 86.4% in the presence of 20% HS (p=0.1574); it decreased to 70.4% in the presence of 50% HS (p=0.0224) (figure 2B, right panel). We observed no significant changes in the titer of SJ-607 virus in the presence of 50% heat-inactivated serum, compared with serum-free conditions (99.5% vs 100.0%; data not shown). In conclusion, the incorporation of human CD55 on the membrane of SJ-600 series viruses, particularly SJ-607, conferred resistance to complement-mediated virus neutralization; thus, it substantially improved viral stability in HS.

In vitro oncolytic activities of SJ-600 series viruses were unaffected by CD55 expression

To investigate whether CD55 expression affected the infectivity and oncolytic activity of SJ-600 series viruses, in vitro cytotoxic effects were compared between SJ-607

and JX-594. Ten human cancer cell lines were infected with serially diluted SJ-607 or JX-594; cell viabilities were measured at 72 hours post-infection by CCK-8 assays. Both SJ-607 and JX-594 viruses effectively killed all examined cancer cells; there were no significant differences in oncolytic effects between the two viruses (figure 2C and online supplemental figure 2). Although the sensitivities of cancer cells to oncolytic VACVs differed among cell lines, the mean EC_{50} values of all 10 cancer cell lines were within the range of 0.0016–0.2805 pfu/cell (online supplemental table 1). These findings indicated that oncolytic VACVs very efficiently infected and killed many types of human cancer cells, confirming the broad spectrum of effects of these viruses.

Systemically administered SJ-607 virus showed improved therapeutic efficacy in vivo

Because human CD55 is functionally cross-reactive with the murine complement system,[35] we investigated the in vivo antitumor efficacy of intravenously administered SJ-607 virus in mice carrying human cancer xenografts. Human colon cancer HCT-116 cells were subcutaneously implanted into NSG mice; the mice underwent intravenous injection of a single dose of SJ-607 or control JX-594 virus at $5×10^6$ pfu when the tumor volume reached 80–100 mm^3 (figure 3A). After systemic administration of SJ-607 virus, the primary tumor mass increased until day 6 of treatment (up to 155 mm^3); it then continuously decreased. Complete remission was observed in most mice on day 22; 94% tumor growth inhibition (TGI) was achieved, compared with vehicle-treated controls (p<0.0001), and the effect was greater than in the JX-594-treated group (p=0.0097) (figure 3B,C). With the exception of one mouse that showed complete remission, the tumor size gradually increased in all mice in the JX-594-treated group; it reached a mean of 250 mm^3 at the end of the experiment (82% TGI compared with vehicle-treated control, p<0.0001) (figure 3B,C). These findings indicated that both SJ-607 and JX-594 viruses very effectively reduced tumor growth in mice carrying human cancer xenografts; the CD55-expressing SJ-607 virus showed a significantly superior oncolytic effect, compared with the control JX-594 virus (p=0.0097).

To evaluate whether the systemic treatment efficacy was dose-dependent, human lung cancer A549 xenografts were intravenously injected one time with LD ($1×10^6$ pfu) or HD ($5×10^6$ pfu) SJ-607 or JX-594 virus when the tumor volume reached 100–120 mm^3 (figure 3D,E). Each group showed considerable TGI: 56% (JX-594, LD), 78% (JX-594, HD), 82% (SJ-607, LD), and 88% (SJ-607, HD); the SJ-607 virus showed superior antitumor efficacy, compared with the control JX-594 virus. The TGI with JX-594 treatment was dependent on the dose administered (LD vs HD: 56% vs 78%, p=0.0035); the SJ-607 virus showed excellent antitumor efficacy at both LDs and HDs (82% and 88%, respectively), with no statistically significant difference between the two doses (figure 3D). Moreover, the TGI was better in the LD SJ-607 group than in the HD JX-594 group (figure 3D), indicating that the SJ-607 virus showed a similar antitumor effect at less than one-fifth of the dose of the JX-594 virus.

To determine whether the SJ-607 virus could effectively inhibit the growth of larger tumors, a single LD or HD of JX-594 or SJ-607 virus ($1×10^6$ pfu or $5×10^6$ pfu, respectively) was intravenously administered into human lung cancer xenografts when the mean tumor volume was 200 mm^3. Surprisingly, a similar pattern of therapeutic efficacy was observed: tumor mass decreased to the initial volume of treatment in both LD and HD SJ-607 groups on day 17, whereas similar effects were observed only in the HD JX-594 group (online supplemental figure 3). These observations indicated that our new oncolytic VACV SJ-607 expressing human CD55 had superior antitumor efficacy, compared with the control JX-594 virus.

In vivo biodistribution and kinetics of systemically administered SJ-607 virus

The above results showed that systemic administration of the SJ-607 virus had superior antitumor efficacy, compared with the control JX-594 virus. To evaluate the biodistribution and kinetics of systemically administered viruses, human colon cancer xenografts were intravenously injected with $1×10^6$ pfu SJ-607 or SJ-610 virus, a control virus without human CD55 but containing the luciferase gene (table 1), when tumor size reached ~200 mm^3. The in vivo biodistribution and kinetics of the viruses were monitored using an imaging system (IVIS Lumina X5; PerkinElmer). At 56 hours post-injection, SJ-607 virus appeared specifically in the tumor site in the right flank; its maximum intensity ($9.18×10^9$ radiance (p/s/cm^2/sr)) was observed at 120 hours (figure 4A and B). Control SJ-610 virus appeared in the tumor site at 96 hours; its maximum intensity was observed at 120 hours ($4.08×10^9$ radiance (p/s/cm^2/sr)), and the intensity subsequently decreased (figure 4A,B, online supplemental table 2). Thus, after intravenous administration, SJ-607 virus appeared earlier, proliferated and persisted for a longer duration, and reached a higher maximum intensity in the tumor site compared with SJ-610 virus; these results suggested that SJ-607 survived better in the circulation, reached the tumor site earlier, and proliferated at the tumor site for an extended period. Moreover, both SJ-607 and SJ-610 viruses showed specific accumulation only in the tumor site after intravenous administration, suggesting that minimal side effects may occur after systemic treatment (online supplemental figure 4).

Next, we analyzed the distribution of oncolytic VACVs in the tumor tissue. Human lung cancer xenografts were intravenously injected with a single dose of $1×10^6$ pfu (LD) of SJ-607 or control SJ-610 virus when the tumor volume reached ~200 mm^3; tumor tissues were sampled after 120 hours and the viral distributions were evaluated by analyses of the green fluorescent protein signal (table 1). The OVs were clustered at multiple loci in the periphery of the tumor tissue; notably, SJ-607 showed widespread invasion throughout the tumor (figure 4C).
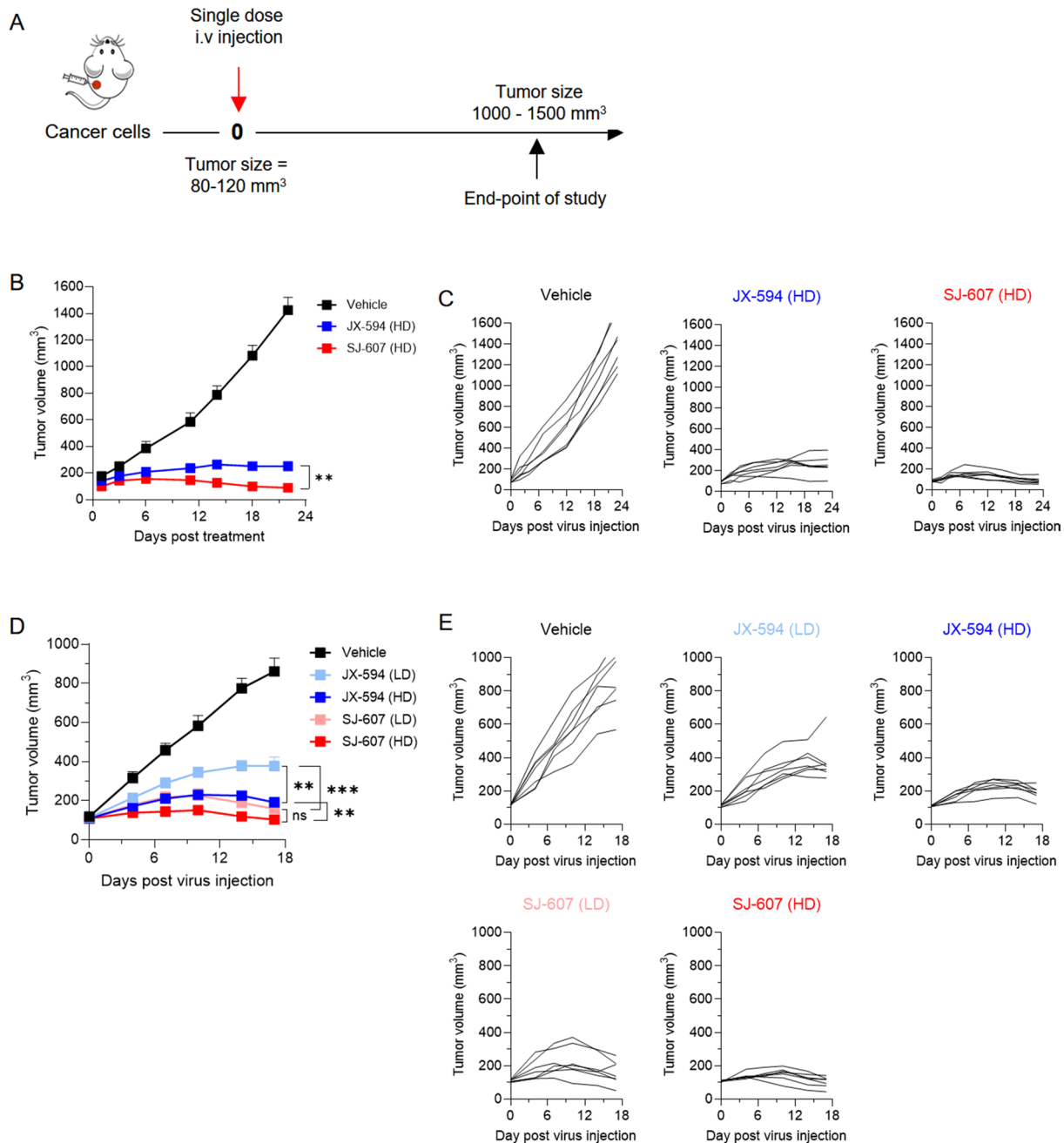
Figure 3 Antitumor efficacy of systemically administered SJ-607 in tumor-bearing mice. Tumor-bearing mice were intravenously injected with a single dose of virus when tumor size was approximately 80–100 mm^3. (A) Schematic of experimental protocol. (B) Tumor growth curve of HCT-116 model. HCT-116 human colon cancer cells were subcutaneously implanted into NSG mice and recombinant vaccinia virus (5×10^6 pfu) was intravenously injected through the tail vein (n=7 mice per group). (C) Individual growth curves of HCT-116-bearing mice. (D) Tumor growth curve of A549 model. A549 human lung cancer cells were subcutaneously implanted into NSG mice and a single dose of recombinant vaccinia virus (high dose, 5×10^6 pfu; low dose, 1×10^6 pfu; n=7 mice per group) was intravenously injected through the tail vein. (E) Individual growth curves of A549-bearing mice. Tumor growth data are presented as means±EM. HD, high dose; i.v., intravenous; LD, low dose; OV, oncolytic virus; TGI, tumor growth inhibition.

The area of the green fluorescent protein signal of the virus was 1.8-fold greater for SJ-607, compared with SJ-610 (figure 4C and D, online supplemental table 3). Thus, the biological basis for the better antitumor efficacy of the new SJ-607 oncolytic VACV platform was the repeated and widespread invasion of tumor tissue by intravenously administered virus.

Systemic administration of SJ-607 virus exhibited better antitumor efficacy, compared with intratumoral treatment

To analyze the antitumor efficacy of the SJ-607 virus according to the route of administration, human triple-negative breast cancer MDA-MB-231 xenografts were intravenously or intratumorally injected with a single dose of 1×10^6 pfu (LD) of SJ-607 or SJ-610 virus when the
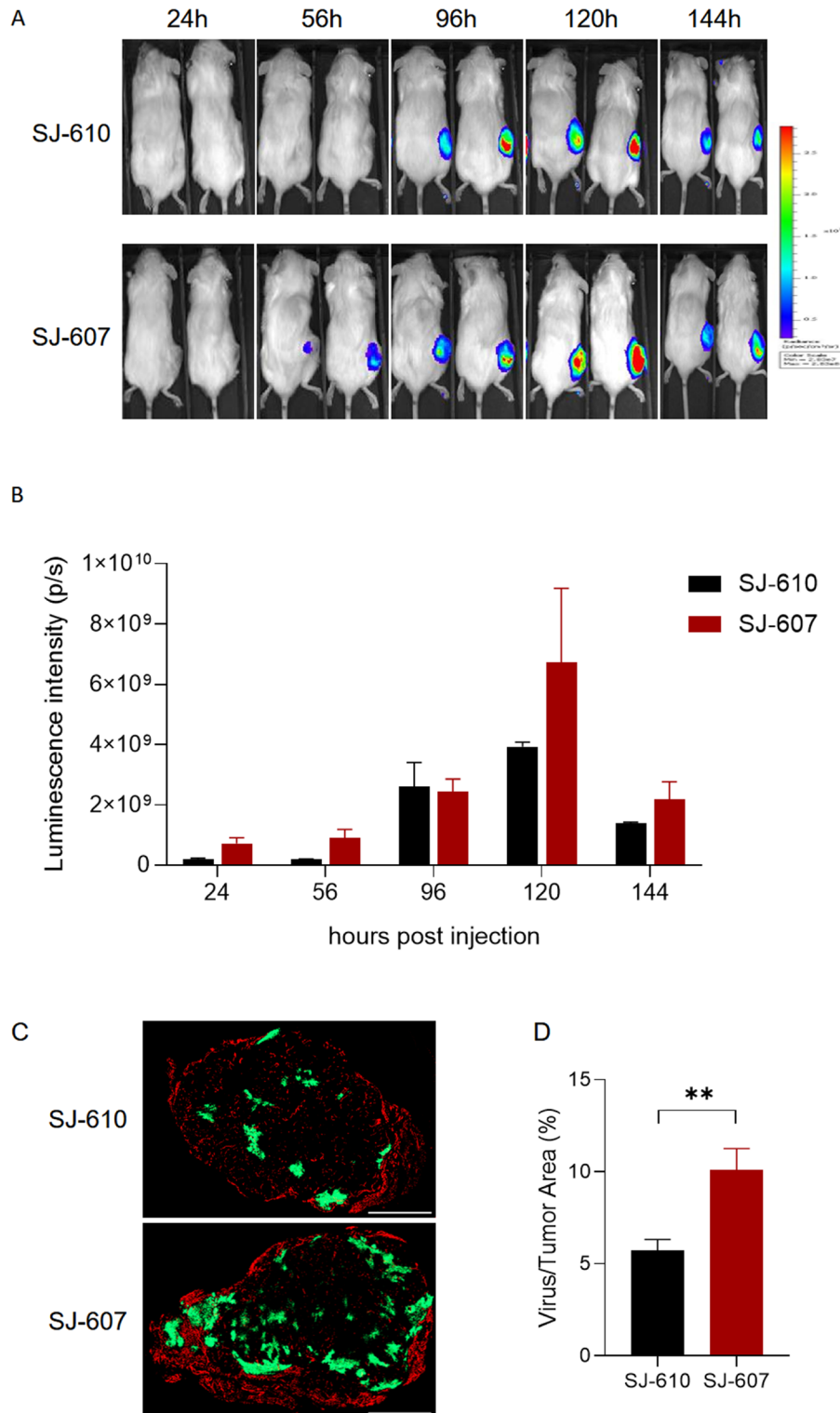
Figure 4 In vivo biodistribution of intravenously injected SJ-607. (A) HCT-116 human colon cancer cells were subcutaneously implanted into NSG mice and a single dose of 1×10^6 pfu SJ-607 or SJ-610 virus was intravenously injected through the tail vein when tumor size was ~200 mm^3. The presence and distribution of virus were analyzed by monitoring luciferase activity using the IVIS system at designated time points. (B) The results are shown as luminescence intensity at 96 hours post-injection (n=2 mice per group) (means±SEM). (C) A549 human lung cancer xenograft NSG mice were intravenously injected with a single dose of SJ-607 or SJ-610 at 1×10^6 pfu when tumor size was ~200 mm^3. The distributions of viral particles in tumor tissue at 120 hours post-injection were analyzed by immunofluorescence. Frozen sections of tumor tissue were labeled with anti-CD31 antibody (red) to visualize blood vessels. Green fluorescent protein was directly expressed by the recombinant viruses. All images were visualized by confocal fluorescence microscopy. Representative and merged images are shown. Scale bars, 2000 µm. (D) Mean area density of viruses in tumors. Data are presented as means±SEM; values were compared using unpaired Student's t-tests. *p<0.05, **p<0.01, ***p<0.001, ****p<0.0001, ns=not significant (p>0.05).
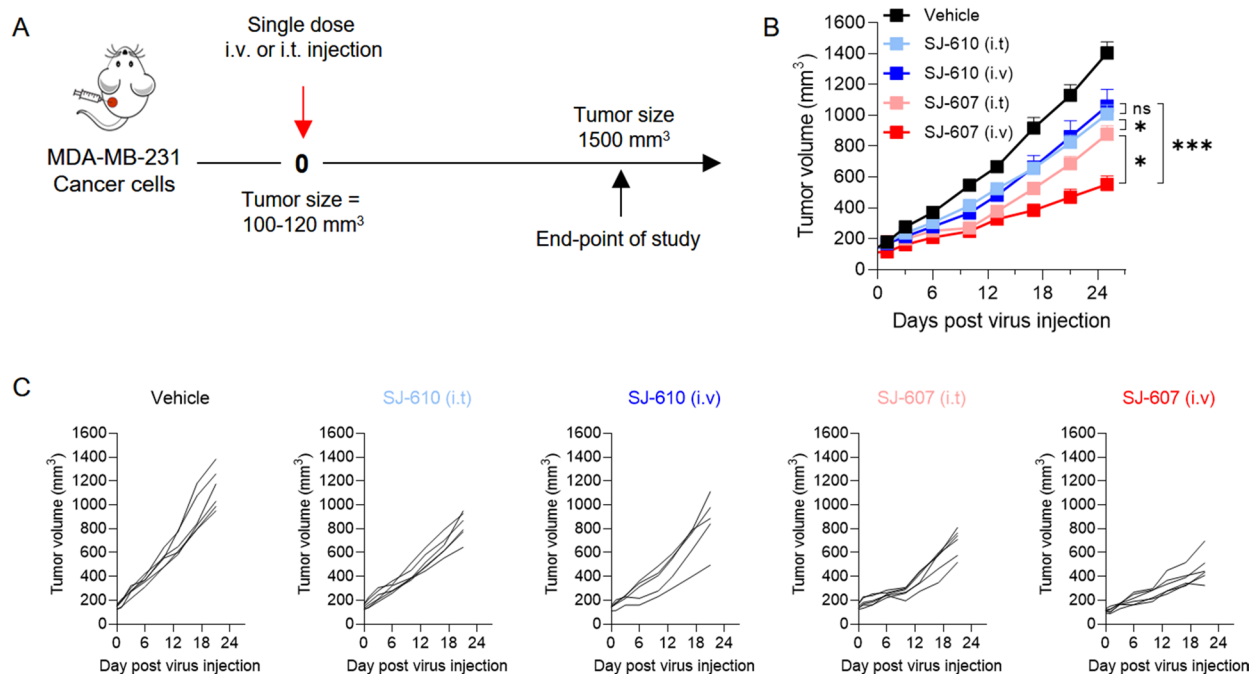
Figure 5 Comparison of antitumor efficacies of systemic versus intratumoral administration of SJ-607. MDA-MB-231 human breast cancer xenografted NSG mice were intratumorally or intravenously injected with a single dose of SJ-600 series virus at 1×10^6 pfu when tumor size was approximately 100–120 mm³; tumor growth was monitored two times weekly (n=5–6 mice per group). (A) Schematic of experimental protocol. (B) Tumor growth curve. (C) Individual tumor growth curves. Tumor growth data are presented as means±SEM. HD, high dose; i.t., intratumoral; i.v., intravenous; LD, low dose; OV, oncolytic virus; TGI, tumor growth inhibition.

tumor volume reached 100–120 mm³ (figure 5A). After systemic treatment, SJ-607 showed significantly better efficacy, compared with the control SJ-610 virus (61% and 25% TGI, respectively; p=0.0002) (figure 5B,C). For the SJ-610 virus, antitumor efficacy was similar between intratumoral and intravenous routes of administration (28% and 25% TGI, respectively) (figure 5B,C). For the human CD55-expressing SJ-607 virus, intravenous treatment resulted in significantly better therapeutic efficacy, than intratumoral treatment (61% and 38% TGI, respectively; p=0.0243) (figure 5B,C). This result was surprizing because intratumoral administration of OV immunotherapy has generally demonstrated better treatment efficacy, compared with intravenous administration.[36] Improved OV survival during systemic circulation could thus improve anticancer efficacy after intravenous administration.

SJ-607 evaded neutralization by VACV-specific antibodies produced after multiple systemic administration of OV

Intratumoral treatment is prevalent in clinical settings, and its antitumor efficacy has been superior to the efficacy of intravenous treatment.[36] In addition to the complement-mediated destruction of circulating virus, the generation of NAb against OVs after repeated treatment can also hinder the treatment efficacy of systemically administered virus.[37–40] Because the complement-mediated immune response affects innate and adaptive immunity,[41] we speculated that evasion of complement-mediated immunity through the expression of CD55 may affect the formation

of antiviral antibodies. We evaluated the production of antibodies specific to the injected virus in two strains of immunocompetent mice.

Female BALB/c and C57BL/6 mice were intravenously injected one time or three times (1/week) with 5×10^6 pfu/dose of SJ-607 virus or control JX-594 virus. Serum was collected before virus injection (baseline) and at 1, 2, 3, 4, and 5 weeks after the first injection (figure 6A). SJ-607 and JX-594 viruses were incubated with serially diluted heat-inactivated serum; serum-treated viruses were incubated with U-2-OS cells for 3 days to evaluate the cytopathic effects. The titer$_{50}$ of NAb against VACV was defined as the reciprocal of the highest dilution of serum that resulted in cell viability ≥50%. At 4–5 weeks after a single dose of JX-594 virus, significant levels of NAb were formed (figure 6B, C, E and F). When multiple doses were administered, the titer of NAb against JX-594 significantly increased from week 2 after the first injection. These findings indicated that NAb to injected virus had already formed by the time of the third virus injection, which would reduce the efficacy of injected OVs (figure 6B, D, E and G).

In contrast, it was observed that serum collected after a single dose (figure 6H, I, K and L) and multiple doses of SJ-607 virus (figure 6H, J, K and M) were unable to neutralize SJ-607 for both BALB/c and C57BL/6 mice. In terms of individual % cell viability, minimal levels of NAb were detected from the third week after the first virus injection in mice that received multiple doses of SJ-607
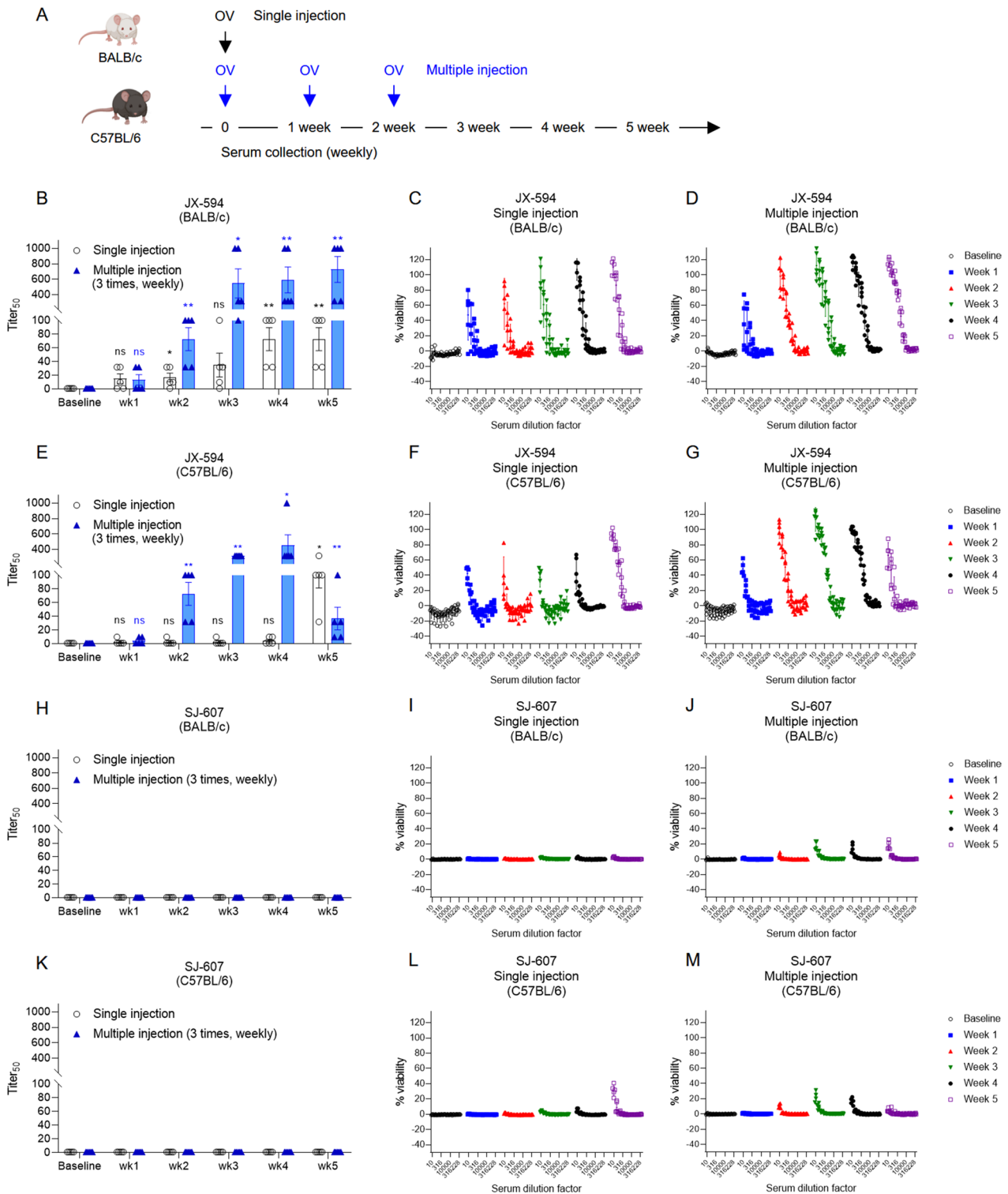
Figure 6 Neutralizing antibody titration in SJ-607-injected mouse serum. Naive (tumor-free) BALB/c or C57BL/6 mice were systemically injected with 5×10^6 pfu of JX-594 or SJ-607 one time or three times weekly; mouse serum was collected prior to the first injection (baseline) and weekly for 5 weeks. The presence of neutralizing antibody against vaccinia virus was determined by neutralizing antibody titer_{50}, defined as the reciprocal of the highest dilution of serum that resulted in cell viability ≥50% (n=5 mice per group). (A) Schematic of experimental protocol. Titer_{50} values of JX-594-injected BALB/c mice (B) and C57BL/6 mice (E), and SJ-607-injected BALB/c mice (H), and C57BL/6 mice (K) are plotted. Experiments were conducted in duplicate, and data are shown as means±SEM of five mice. Individual % viabilities of U-2-OS cells infected with JX-594 or SJ-607 incubated with serially diluted mouse serum collected at each time point are presented on the right. (C, D) JX-594-injected BALB/c mice, (F, G) JX-594-injected C57BL/6 mice, (I, J) SJ-607-injected BALB/c mice, and (L, M) SJ-607-injected C57BL/6 mice. Unpaired Student's t-tests were used for comparisons with baseline control. $p<0.05$ (*), $p<0.01$ (**), ns=not significant. OV, oncolytic virus.
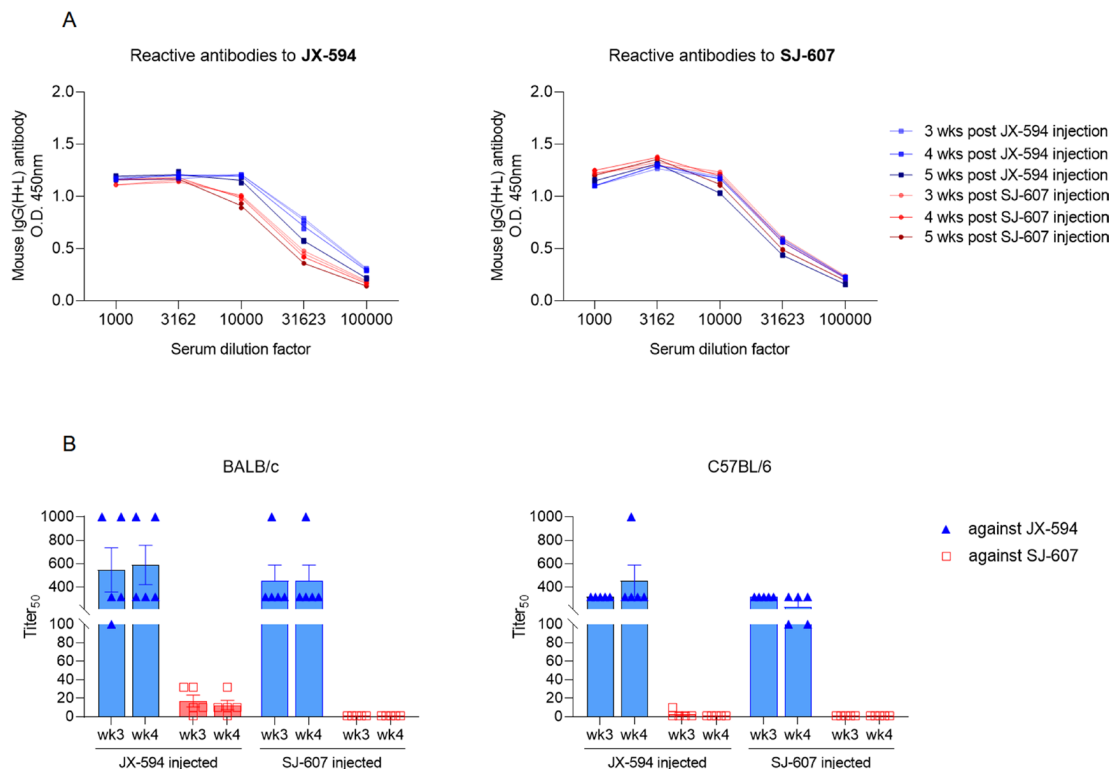
Figure 7 Titration of total reactive antibody and neutralizing antibody in JX-594 or SJ-607 injected mouse serum. Naïve (tumor-free) BALB/c or C57BL/6 mice were systemically injected with 5×10^6 pfu of JX-594 or SJ-607 three times weekly via tail vein; mouse serum was collected weekly for 5 weeks after the first injection. (A) The presence of total vaccinia virus reactive antibodies to JX-594 or SJ-607 in BALB/c mouse serum at 3, 4, and 5 weeks following the first OV treatment was measured using the ELISA method. Intact JX-594 or SJ-607 viruses were coated on the 96-well plates and heat-inactivated mouse serum was treated as primary antibody. Detection was performed using HRP-conjugated anti-mouse IgG secondary antibody at 450 nm to quantitate the total antibodies reactive to JX-594 (left) or SJ-607 (right). (B) The neutralizing activity against JX-594 or SJ-607 was determined. Serially diluted, heat-inactivated mouse serum at 3 and 4 weeks following the first OV treatment were incubated with JX-594 or SJ-607 and transferred onto cultures of U-2 OS cells. Neutralizing activity in BABL/c mouse (left) and C57BL/6 mice (right) are shown. OV, oncolytic virus.

virus; these levels did not increase until the fifth week (figure 6J,M). Next, we sought to determine whether antibodies against SJ-607 were generated by measuring the total VACV reactive antibodies from the serum of mice injected with either SJ-607 or JX-594 virus multiple times. Briefly, intact JX-594 or SJ-607 viruses were coated on the plate and heat-inactivated virus-treated mouse serum was used as the primary antibody. HRP-conjugated anti-mouse IgG antibody was used as the secondary antibody to quantitate the total antibody reactive to JX-594 or SJ-607 virus. The total amount of VACV-reactive antibodies to surface proteins of JX-594 and that of SJ-607 in serum were similar (figure 7A). Hence, intravenous administration of oncolytic VACV induced a similar level of total VACV reactive antibodies irrespective of human CD55 molecule incorporation on IMV membrane.

To evaluate whether the antibodies formed in the SJ-607-treated mice could neutralize VACV or whether SJ-607 avoided neutralization by antibodies, serum from SJ-607-treated mice was incubated with JX-594 virus and serum from JX-594-treated mice was incubated with SJ-607 virus, respectively. Then the neutralizing activity was measured in the same way as described above. Serum

from SJ-607-treated mice was able to neutralize JX-594 virus, almost equivalent to that by serum from JX-594-treated mice. However, serum from JX-594-treated mice could not neutralize SJ-607 virus as like a serum from SJ-607-treated mice could not (figure 7B). These results imply the formation of NAbs against VACV in SJ-607-treated mice, but SJ-607 can evade neutralization by VACV-specific antibodies, which is a trait unobserved in JX-594. From these observations, it was inferred that our new SJ-607 virus could provide sustainable antitumor activity with a repeated systemic treatment regimen by evading neutralization by VACV-specific antibodies produced after multiple administration of OVs.

DISCUSSION
Intravenous treatment with human CD55-expressing SJ-607 virus increased anticancer activity in three human cancer xenografts, compared with the control JX-594 virus. In this study, we show that intravenous administration of human CD55-expressing SJ-607 virus increases anticancer activity in three different human cancer xenografts, when compared with the control JX-594.

Additionally, we observed SJ-607 could evade neutralization by VACV-specific antibodies formed after single and multiple instances of systemic treatment with OV, in contrast to susceptibility of JX-594 to NAb.

The incorporation levels of human CD55 fusion protein on the IMV membrane in SJ-600 series viruses were closely correlated with the inherent abundance of fusion partner viral proteins (H3 > D8 > F9 > L1 > A16 > G9) (SJ-607 > SJ-601 > SJ-605 > SJ-608 > SJ-604 > SJ-606).[28] The serum stability was also correlated with the incorporation level, with the exception of SJ-601 (figure 2A). Two forms of virus-expressed human CD55 protein were identified; their molecular weights were 50 kDa and 70 kDa, depending on the glycosylation status (figure 1C). In SJ-601, we fused CD55 with D8, which was highly incorporated on the VACV membrane. However, human CD55 was not glycosylated on SJ-601 (only the 50 kDa band was present); its susceptibility was similar to JX-594, which did not express human CD55 on the membrane. These observations indicated that CD55 requires glycosylation for proper function. Because the proteins of VACV IMVs are not glycosylated, the glycosylation process of the CD55 fusion protein during IMV morphogenesis, which was compromised in SJ-601, may have affected the glycosylation status of CD55 expressed on the membrane.

The SJ-600 series and JX-594 viruses are based on the Wyeth strain VACV, which has been used as a smallpox vaccine platform.[32] However, because the oncolytic activity of the Wyeth strain was lower against murine cancer cells than against human cancer cells, we examined the in vivo serum stability and antitumor efficacy of SJ-600 series viruses in human cancer xenograft models that had been established in immunocompromised mice. The essential characteristics of an ideal OV are initial debulking of the tumor mass through effective oncolysis, followed by activation of adaptive immunity to ensure systemic propagation of cancer-specific immunity. Because the NSG mice used as xenograft recipients are deficient in both T and B cells and have minimal natural killer cell activity,[42] this model entirely depends on effective oncolysis and innate immunity without natural killer cells. Even in this scenario, the SJ-607-treated group was significantly superior to the control JX-594-treated group for efficacy in all three human cancer xenografts. Further evaluation of the full immuno-oncological capability of human CD55-expressing oncolytic VACV in a fully immunocompetent context is needed to assess the cell-mediated and antibody-mediated immunities induced by SJ-600 series viruses. Additionally, the strength and kinetics of immune responses against viral antigens versus cancer antigens are crucial considerations; the relative response kinetics can affect the initial viral spread and subsequent potent anticancer immune activation, as well as eventual long-term immune memory formation. This information will help to characterize our new oncolytic VACV platform and may improve its clinical translation potential for use in human patients.

Previous human trials of Pexa-Vec oncolytic viral therapy have reported that repeated administration of virus elicits antiviral NAb within 3 weeks[37 38] which limits the window of effectiveness to a short time period. For translation into an immunocompetent context, we examined whether multiple doses of SJ-607 virus could induce NAb against the injected virus in immunocompetent mice. Administration of SJ-607 virus elicited NAb formation against IMV form of VACV absent of CD55 in immunocompetent mice (online supplemental figure 5). Surprisingly, the induced antibodies were not as effective at neutralizing SJ-607. So far, six proteins (H3, D8, L1, A17, A27, A28) have been identified as antigens that induce NAbs to IMV.[43] It can be inferred that these antibodies were formed after SJ-607 administration as the SJ-607 injected mouse serum could neutralize JX-594 (figure 7). Among these antigens, the major immunodominant targets are H3, D8, and L1.[44–46] In addition to the inhibition of neutralization by the function of expressed CD55 molecules on the SJ-607 viruses, it is speculated that NAb might not function effectively enough to suppress the viral infection since CD55 protein was incorporated on the SJ-607 viruses by fusion of CD55 and H3, providing fewer epitopes on the surface of IMV to which antibodies can bind. Therefore, in contrast to other OVs, SJ-607 will be less affected by antibodies, enabling sustained delivery to tumor tissue even after repeated injection in an immunocompetent host. Also it is important to evaluate when cell-mediated and antibody-mediated antiviral immune responses occur after SJ-607 administration,[47] which will affect clearance of the injected virus. Further studies of the eventual balance and kinetics of immunity against viral antigens and cancer antigens are also needed because these processes strongly influence both initial oncolysis and eventual systemic antitumor immunity, which clearly determine treatment efficacy and patient outcomes.

There have been multiple attempts to prolong the duration of viral circulation after intravenous injection for OV immunotherapy.[1 48] There have also been reports of successful systemic treatment using engineered OVs.[49 50] Because the extracellular enveloped or 'cloaked' form of VACV facilitates widespread dissemination,[51] systemic administration of VACVs has been partly successful in both preclinical and clinical studies[37 52]; further modifications have been reported that involve deletion of B5R, the major target protein for extracellular enveloped virion NAb,[53] and the addition of PI3Kδ inhibitor to prevent phagocytosis.[54 55] Our new platform incorporating human CRP CD55 on IMVs demonstrated excellent anticancer efficacy, even with single-dose intravenous administration in immunocompromised mice. With the aid of the intact immune system in immunocompetent hosts and in combination with immune checkpoint blockade, our novel platform could be active until achievement of the complete remission of multiple widespread and heterogeneous tumors. Further studies are needed to determine whether our new oncolytic VACV has ideal OV characteristics, including initial immune evasion to prolong the

duration of viral circulation and thus increase oncolysis; subsequent antiviral immunity to clear the virus; and finally anticancer immune activation to enhance the effector T-cell response, thus eradicating cancer cells and promoting the formation of memory T cells that can prevent recurrence.

Author affiliations
[1] Research Center, SillaJen, Inc, Seongnam, Gyeonggi-do, Republic of Korea
[2] Department of Biomedical Sciences, Seoul National University College of Medicine, Seoul, Republic of Korea
[3] Wide River Institute of Immunology, Seoul National University, Gangwon, Republic of Korea

ORCID iD
Dong-Sup Lee http://orcid.org/0000-0001-8312-2705

REFERENCES

1. Kaufman HL, Kohlhapp FJ, Zloza A. Oncolytic viruses: a new class of immunotherapy drugs. *Nat Rev Drug Discov* 2015;14:642–62.
2. Ribas A, Dummer R, Puzanov I, *et al*. Oncolytic virotherapy promotes intratumoral T cell infiltration and improves anti-PD-1 immunotherapy. *Cell* 2017;170:1109–19.
3. Jeon Y-H, Lee N, Yoo J, *et al*. Oncolytic vaccinia virus augments T cell factor 1-positive stem-like CD8+ T cells, which underlies the efficacy of anti-PD-1 combination immunotherapy. *Biomedicines* 2022;10:805
4. Chon HJ, Lee WS, Yang H, *et al*. Tumor microenvironment remodeling by intratumoral oncolytic vaccinia virus enhances the efficacy of immune-checkpoint blockade. *Clin Cancer Res* 2019;25:1612–23.
5. Martin NT, Bell JC. Oncolytic virus combination therapy: killing one bird with two stones. *Mol Ther* 2018;26:1414–22.
6. Bommareddy PK, Shettigar M, Kaufman HL. Integrating oncolytic viruses in combination cancer immunotherapy. *Nat Rev Immunol* 2018;18:498–513.
7. Russell SJ, Barber GN. Oncolytic viruses as antigen-agnostic cancer vaccines. *Cancer Cell* 2018;33:599–605.
8. Russell SJ, Peng KW, Bell JC. Oncolytic virotherapy. *Nat Biotechnol* 2012;30:658–70.
9. Andtbacka RHI, Kaufman HL, Collichio F, *et al*. Talimogene laherparepvec improves durable response rate in patients with advanced melanoma. *J Clin Oncol* 2015;33:2780–8.
10. Nakao S, Arai Y, Tasaki M, *et al*. Intratumoral expression of IL-7 and IL-12 using an oncolytic virus increases systemic sensitivity to immune checkpoint blockade. *Sci Transl Med* 2020;12:eaax7992
11. Melero I, Castanon E, Alvarez M, *et al*. Intratumoural administration and tumour tissue targeting of cancer immunotherapies. *Nat Rev Clin Oncol* 2021;18:558–76.
12. Hammerich L, Bhardwaj N, Kohrt HE, *et al*. In situ vaccination for the treatment of cancer. *Immunotherapy* 2016;8:315–30.
13. Hammerich L, Marron TU, Upadhyay R, *et al*. Systemic clinical tumor regressions and potentiation of PD1 blockade with in situ vaccination. *Nat Med* 2019;25:814–24.
14. Jahan N, Ghouse SM, Martuza RL, *et al*. In situ cancer vaccination and immunovirotherapy using oncolytic HSV. *Viruses* 2021;13:1740
15. Breitbach CJ, Lichty BD, Bell JC. Oncolytic viruses: therapeutics with an identity crisis. *EBioMedicine* 2016;9:31–6.
16. Seymour LW, Fisher KD. Oncolytic viruses: finally delivering. *Br J Cancer* 2016;114:357–61.
17. Easwaran H, Tsai H-C, Baylin SB. Cancer epigenetics: tumor heterogeneity, plasticity of stem-like states, and drug resistance. *Mol Cell* 2014;54:716–27.
18. Hausser J, Alon U. Tumour heterogeneity and the evolutionary trade-offs of cancer. *Nat Rev Cancer* 2020;20:247–57.
19. Vitale I, Shema E, Loi S, *et al*. Intratumoral heterogeneity in cancer progression and response to immunotherapy. *Nat Med* 2021;27:212–24.
20. Russell SJ, Bell JC, Engeland CE, *et al*. Advances in oncolytic virotherapy. *Commun Med (Lond)* 2022;2:33
21. Ostrycharz E, Hukowska-Szematowicz B. New insights into the role of the complement system in human viral diseases. *Biomolecules* 2022;12:226
22. Ander SE, Li FS, Carpentier KS, *et al*. Innate immune surveillance of the circulation: a review on the removal of circulating virions from the bloodstream. *PLoS Pathog* 2022;18:e1010474
23. Smith GL, Vanderplasschen A, Law M. The formation and function of extracellular enveloped vaccinia virus. *J Gen Virol* 2002;83:2915–31.
24. Roberts KL, Smith GL. Vaccinia virus morphogenesis and dissemination. *Trends Microbiol* 2008;16:472–9.
25. Vanderplasschen A, Mathew E, Hollinshead M, *et al*. Extracellular enveloped vaccinia virus is resistant to complement because of incorporation of host complement control proteins into its envelope. *Proc Natl Acad Sci U S A* 1998;95:7544–9.
26. Bernet J, Mullick J, Singh AK, *et al*. Viral mimicry of the complement system. *J Biosci* 2003;28:249–64.
27. Chung C-S, Chen C-H, Ho M-Y, *et al*. Vaccinia virus proteome: identification of proteins in vaccinia virus intracellular mature virion particles. *J Virol* 2006;80:2127–40.
28. Embry A, Meng X, Cantwell A, *et al*. Enhancement of immune response to an antigen delivered by vaccinia virus by displaying the antigen on the surface of intracellular mature virion. *Vaccine* 2011;29:5331–9.
29. Park B-H, Hwang T, Liu T-C, *et al*. Use of a targeted oncolytic poxvirus, JX-594, in patients with refractory primary or metastatic liver cancer: a phase I trial. *Lancet Oncol* 2008;9:533–42.
30. Heo J, Reid T, Ruo L, *et al*. Randomized dose-finding clinical trial of oncolytic immunotherapeutic vaccinia JX-594 in liver cancer. *Nat Med* 2013;19:329–36.
31. Mackett M, Smith GL, Moss B. Vaccinia virus: a selectable eukaryotic cloning and expression vector. *Proc Natl Acad Sci U S A* 1982;79:7415–9.

32 Mastrangelo MJ, Maguire HC, Eisenlohr LC, *et al*. Intratumoral recombinant GM-CSF-encoding virus as gene therapy in patients with cutaneous melanoma. *Cancer Gene Ther* 1999;6:409–22.

33 Cotter CA, Earl PL, Wyatt LS, *et al*. Preparation of cell cultures and vaccinia virus stocks. *Curr Protoc Microbiol* 2015;39:14A.

34 Moss B. Poxvirus cell entry: how many proteins does it take? *Viruses* 2012;4:688–707.

35 Harris CL, Spiller OB, Morgan BP. Human and rodent decay-accelerating factors (CD55) are not species restricted in their complement-inhibiting activities. *Immunology* 2000;100:462–70.

36 Macedo N, Miller DM, Haq R, *et al*. Clinical landscape of oncolytic virus research in 2020. *J Immunother Cancer* 2020;8:e001486

37 Breitbach CJ, Burke J, Jonker D, *et al*. Intravenous delivery of a multi-mechanistic cancer-targeted oncolytic poxvirus in humans. *Nature* 2011;477:99–102.

38 Evgin L, Acuna SA, Tanese de Souza C, *et al*. Complement inhibition prevents oncolytic vaccinia virus neutralization in immune humans and cynomolgus macaques. *Mol Ther* 2015;23:1066–76.

39 Fisher KD, Stallwood Y, Green NK, *et al*. Polymer-Coated adenovirus permits efficient retargeting and evades neutralising antibodies. *Gene Ther* 2001;8:341–8.

40 Mace ATM, Ganly I, Soutar DS, *et al*. Potential for efficacy of the oncolytic herpes simplex virus 1716 in patients with oral squamous cell carcinoma. *Head Neck* 2008;30:1045–51.

41 Carroll MC. The complement system in regulation of adaptive immunity. *Nat Immunol* 2004;5:981–6.

42 Ito M, Hiramatsu H, Kobayashi K, *et al*. NOD/SCID/gamma(c)(null) mouse: an excellent recipient mouse model for engraftment of human cells. *Blood* 2002;100:3175–82.

43 Shchelkunov SN, Shchelkunova GA. Genes that control vaccinia virus immunogenicity. *Acta Naturae* 2020;12:33–41.

44 Davies DH, McCausland MM, Valdez C, *et al*. Vaccinia virus H3L envelope protein is a major target of neutralizing antibodies in humans and elicits protection against lethal challenge in mice. *J Virol* 2005;79:11724–33.

45 Pulford DJ, Gates A, Bridge SH, *et al*. Differential efficacy of vaccinia virus envelope proteins administered by DNA immunisation in protection of balb/c mice from a lethal intranasal poxvirus challenge. *Vaccine* 2004;22:3358–66.

46 Fogg C, Lustig S, Whitbeck JC, *et al*. Protective immunity to vaccinia virus induced by vaccination with multiple recombinant outer membrane proteins of intracellular and extracellular virions. *J Virol* 2004;78:10230–7.

47 Liu J, Miwa T, Hilliard B, *et al*. The complement inhibitory protein DAF (CD55) suppresses T cell immunity in vivo. *J Exp Med* 2005;201:567–77.

48 Ban W, Guan J, Huang H, *et al*. Emerging systemic delivery strategies of oncolytic viruses: a key step toward cancer immunotherapy. *Nano Res* 2022;15:4137–53.

49 Naik S, Nace R, Federspiel MJ, *et al*. Curative One-shot systemic virotherapy in murine myeloma. *Leukemia* 2012;26:1870–8.

50 Russell SJ, Federspiel MJ, Peng K-W, *et al*. Remission of disseminated cancer after systemic oncolytic virotherapy. *Mayo Clin Proc* 2014;89:926–33.

51 Kirn DH, Wang Y, Liang W, *et al*. Enhancing poxvirus oncolytic effects through increased spread and immune evasion. *Cancer Res* 2008;68:2071–5.

52 Park JS, Lee ME, Jang WS, *et al*. Systemic injection of oncolytic vaccinia virus suppresses primary tumor growth and lung metastasis in metastatic renal cell carcinoma by remodeling tumor microenvironment. *Biomedicines* 2022;10:173

53 Bell E, Shamim M, Whitbeck JC, *et al*. Antibodies against the extracellular enveloped virus B5R protein are mainly responsible for the EEV neutralizing capacity of vaccinia immune globulin. *Virology* 2004;325:425–31.

54 Ferguson MS, Chard Dunmall LS, Gangeswaran R, *et al*. Transient inhibition of PI3Kδ enhances the therapeutic effect of intravenous delivery of oncolytic vaccinia virus. *Mol Ther* 2020;28:1263–75.

55 Marelli G, Chard Dunmall LS, Yuan M, *et al*. A systemically deliverable vaccinia virus with increased capacity for intertumoral and intratumoral spread effectively treats pancreatic cancer. *J Immunother Cancer* 2021;9:e001624